

Effect of laser annealing of pressure gradients in a diamond-anvil cell using common solid pressure media

Ilya Uts, Konstantin Glazyrin, and Kanani K. M. Lee

Citation: *Rev. Sci. Instrum.* **84**, 103904 (2013); doi: 10.1063/1.4821620

View online: <http://dx.doi.org/10.1063/1.4821620>

View Table of Contents: <http://rsi.aip.org/resource/1/RSINAK/v84/i10>

Published by the [AIP Publishing LLC](#).

Additional information on *Rev. Sci. Instrum.*

Journal Homepage: <http://rsi.aip.org>

Journal Information: http://rsi.aip.org/about/about_the_journal

Top downloads: http://rsi.aip.org/features/most_downloaded

Information for Authors: <http://rsi.aip.org/authors>



New, Easy-to-Mount
FLIR A6700sc Camera

When you need Science-Grade IR in Tight Spaces

FLIR

Get Datasheet 

The advertisement features a black FLIR A6700sc camera with a lens and a FLIR logo on its side, positioned in front of a colorful, glowing circuit board. The background is dark blue with a subtle pattern of circuit traces.

Effect of laser annealing of pressure gradients in a diamond-anvil cell using common solid pressure media

Ilya Uts,^{1,2} Konstantin Glazyrin,^{1,3,a)} and Kanani K. M. Lee^{1,a)}

¹*Department of Geology & Geophysics, Yale University, New Haven, Connecticut 06511, USA*

²*Department of Astronomy, Yale University, New Haven, Connecticut 06511, USA*

³*FS-PE Group, PETRA-3, Deutsches Elektronen-Synchrotron Ein Forschungszentrum der Helmholtz-Gemeinschaft (DESY), Hamburg 22607, Germany*

(Received 17 May 2013; accepted 4 September 2013; published online 4 October 2013)

Pressure media are one of the most effective deterrents of pressure gradients in diamond-anvil cell (DAC) experiments. The media, however, become less effective with increasing pressure, particularly for solid pressure media. One of the most popular ways of alleviating the increase in pressure gradients in DAC samples is through laser annealing of the sample. We explore the effectiveness of this technique for six common solid pressure media that include: alkali metal halides LiF, NaCl, KCl, CsCl, KBr, as well as amorphous SiO₂. Pressure gradients are determined through the analysis of the first-order diamond Raman band across the sample before and after annealing the sample with a near-infrared laser to temperatures between ~2000 and 3000 K. As expected, we find that in the absence of sample chamber geometrical changes and diamond anvil damage, laser annealing reduces pressure gradients, albeit to varying amounts. We find that under ideal conditions, NaCl provides the best deterrent to pressure gradients before and after laser annealing, at least up to pressures of 60 GPa and temperatures between ~2000 and 3000 K. Amorphous SiO₂, on the other hand, transforms in to harder crystalline stishovite upon laser annealing at high pressures resulting in increased pressure gradients upon further compression without laser annealing. © 2013 AIP Publishing LLC. [<http://dx.doi.org/10.1063/1.4821620>]

I. INTRODUCTION

Pressure is one of the most important thermodynamic parameters and strictly corresponds to hydrostatic conditions and to reproduce such conditions has been a goal for high-pressure experimentalists since the inception of high-pressure research.^{1,2} Such pressures are essential in the exploration of various materials, including fluids and solids, especially as they relate to planetary interiors. One common tool for producing high pressures is the diamond-anvil cell. However, the diamond-anvil cell (DAC) is a device that intrinsically applies a uniaxial load. To alleviate some of the non-hydrostaticity inherent in opposed-anvil designs, samples are embedded in a pressure medium. Ideally, this medium is a fluid^{2–6} (i.e., cryogenically cooled or pressurized gases and liquids), but all of these fluids eventually solidify and become nonhydrostatic to a degree. Alternatively, “soft” solid pressure media are employed which can develop substantial pressure gradients as the pressure is increased.^{7,8} Additionally, annealing the sample with a continuous-wave (CW) infrared laser, while under high pressures, has become a common way to reduce pressure gradients.⁷ In this paper, we present a systematic study of several common solid pressure media (e.g., alkali metal halides LiF, NaCl, KCl, CsCl, KBr, and amorphous SiO₂ (*a*-SiO₂)) that are currently used in DAC experiments and discuss the effectiveness of laser heating on annealing these samples up to 60 GPa. The data were obtained by the same procedures

for all of the samples, which allows for a direct comparison between the different pressure media.

While hydrostaticity is generally considered a function of macro stresses (e.g., pressure gradients and deviatoric stress) and micro stresses (e.g., inter-grain stresses), in this study, we are unable to tease out the various components. Thus, we will measure the pressure gradients that are manifested while our samples are under compression. We also note that while pressure is only properly defined for hydrostatic conditions, in this article we shall use the term “pressure” for stress when there are non-hydrostatic conditions.

II. EXPERIMENTAL METHODS

In order to quantify how effective laser annealing is at reducing pressure gradients in DAC samples, we tested several solid pressure media. Each sample consisted of a pair of foils of pressure media (e.g., LiF, NaCl, KCl, CsCl, KBr, and *a*-SiO₂, Table I) surrounding an Fe₂O₃ or Pt foil used as a laser absorber for the alkali halides and *a*-SiO₂, respectively, each foil <5–7 μm thick (Fig. 1). The pressure media additionally acted as thermal insulation between the anvils and the heated laser absorber. The sample sandwich was placed in between a pair of low-fluorescence Type Ia diamond anvils with culets 200 μm in diameter and into a 80–100 μm diameter hole at the center of a pre-indented (30–40 μm thick) Re gasket. To minimize water contamination, the pressure media were placed in a furnace at a temperature of ~400 K before the sample was compressed in the DAC. Although measuring pressure by ruby fluorescence⁹ is commonplace, we do not

^{a)}Authors to whom correspondence should be addressed. Electronic addresses: konstantin.glazyrin@gmail.com and kanani.lee@yale.edu

TABLE I. The room-pressure melting temperatures, bulk (K) and shear (G) moduli are listed for pressure media used. For values not available, NA is listed. Crystal structure designations or mineral names of the materials are included for both low- and high-pressure phases, if relevant for pressure range investigated. Room-pressure melting temperature values, where available and unless otherwise noted, are taken from Ref. 16. High-pressure melting temperature values, where available and unless otherwise noted, are estimated from Ref. 17. Bulk and shear modulus values, unless otherwise noted, are taken from Table 18.5 of Ref. 18. Uncertainties, where available, are listed in parentheses.

Pressure medium	T_{melt} at room pressure (K)	T_{melt} at 60 GPa (K)	K (GPa)	G (GPa)	Reference
LiF (B1)	1121	2900	72.3	48.5	
NaCl (B1)	1074	NA	25.2	14.8	
NaCl (B2)	NA	3250	36.2 (4.2) ^a	NA	14
KCl (B1)	1044	NA	18.1	9.3	
KCl (B2)	NA	3600	28.7 (0.6) ^a	6.25	19 and 20
KBr (B1)	1007	NA	15.0	7.9	
KBr (B2)	NA	3600	14.9 ^b	5.08	15 and 20
CsCl (B2)	919	NA	18.2	10.1	
α -SiO ₂	1480 ^c	NA	36.9	30.9	21
SiO ₂ (stishovite)	NA	~4400	316 (4)	220 (3)	22 and 23

^a Assuming a Birch-Murnaghan equation of state²⁴ and a pressure derivative of the bulk modulus held constant $K_0' = 4$.

^b Assuming a Rydberg-Vinet equation of state²⁵ with a pressure derivative of the bulk modulus held constant $K_0' = 5.81$.

^c Glass transition temperature as given by Ref. 26.

employ ruby in our samples to avoid potential reactions between the ruby and laser absorber and/or pressure medium. We instead measure the Raman signal of diamond¹⁰ to determine pressures using a HORIBA Jobin Yvon LabRAM HR-800 equipped with a 532 nm green laser, 1800 groves/mm grating, 300 μm spectrograph entrance confocal hole and 200 μm slit. As the pressure is determined by the diamond anvil Raman signal, it is imperative that anvils are free from any defects such as scratches or fractures. All Raman measurements were taken at room temperature. Although the use of diamond Raman to measure pressure gradients in DAC samples is not common, we find it can be used effectively to measure pressure gradients.

Upon sample loading, the pressure was increased in increments of ~ 10 GPa and measured in a 3×3 grid across the center of the sample (resulting in 9 measurement points), careful to stay clear of the gasket edge. Distances between the furthest points are ~ 50 μm (Fig. 1). The location of each pressure measurement remained unchanged throughout each compression step. The pressure was averaged and the standard deviation of the pressure across the sample – an indicator for the macro and micro stresses present and thus hydro-

staticity – was determined. The value of the standard deviation yields the level of non-hydrostaticity: the larger the standard deviation, the larger the non-hydrostaticity. At ~ 30 and 60 GPa, we laser annealed to temperatures of ~ 2000 – 3000 K by rastering a 100 W near-infrared (1070 nm) fiber laser as measured by spectroradiometry¹¹ across the sample chamber, three times in increments of 180 s each. Temperatures during annealing fluctuated no more than a few 100 K due to laser absorber distribution throughout the sample chamber. Annealing temperatures for most pressure media tested are lower than their respective melting temperatures, at least where known (Table I). After each single-sided laser annealing, the pressure was determined via diamond Raman across the sample. Additionally, we use the Raman signal of diamond to characterize pressure across the anvil's entire culet and within the anvil to identify internal fractures within the anvils.

Another common solid pressure medium used in high-pressure experiments is MgO. We found, however, that laser annealing often turns to runaway heating and results most often in broken anvils. As such, we have not included MgO in this study.

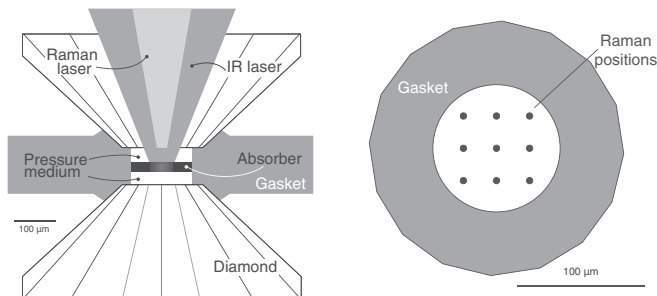


FIG. 1. Sample assembly for all sets of DAC experiments. (Left) Pressure media foils sandwich a thin layer of laser absorber. Annealing was done by a near-IR laser through the top diamond. We used Re gaskets. (Right) Map view of measurement positions within each sample.

III. RESULTS

A. LiF

Initial cold compression of the LiF sample resulted in an expected increase in standard deviation (Fig. 2(a)). Annealing the sample at ~ 30 GPa resulted in a decrease of standard deviation by $\sim 50\%$. Post-annealing compression did not appear to significantly alter the standard deviation within the sample chamber. Instead, the standard deviation remained unaltered after the first heating of 180 s at ~ 60 GPa, and slightly increased after the second 180 s of annealing, as is shown on the right side of Fig. 2(a). An increase of the gasket hole diameter was observed during the second 180 s of heating.

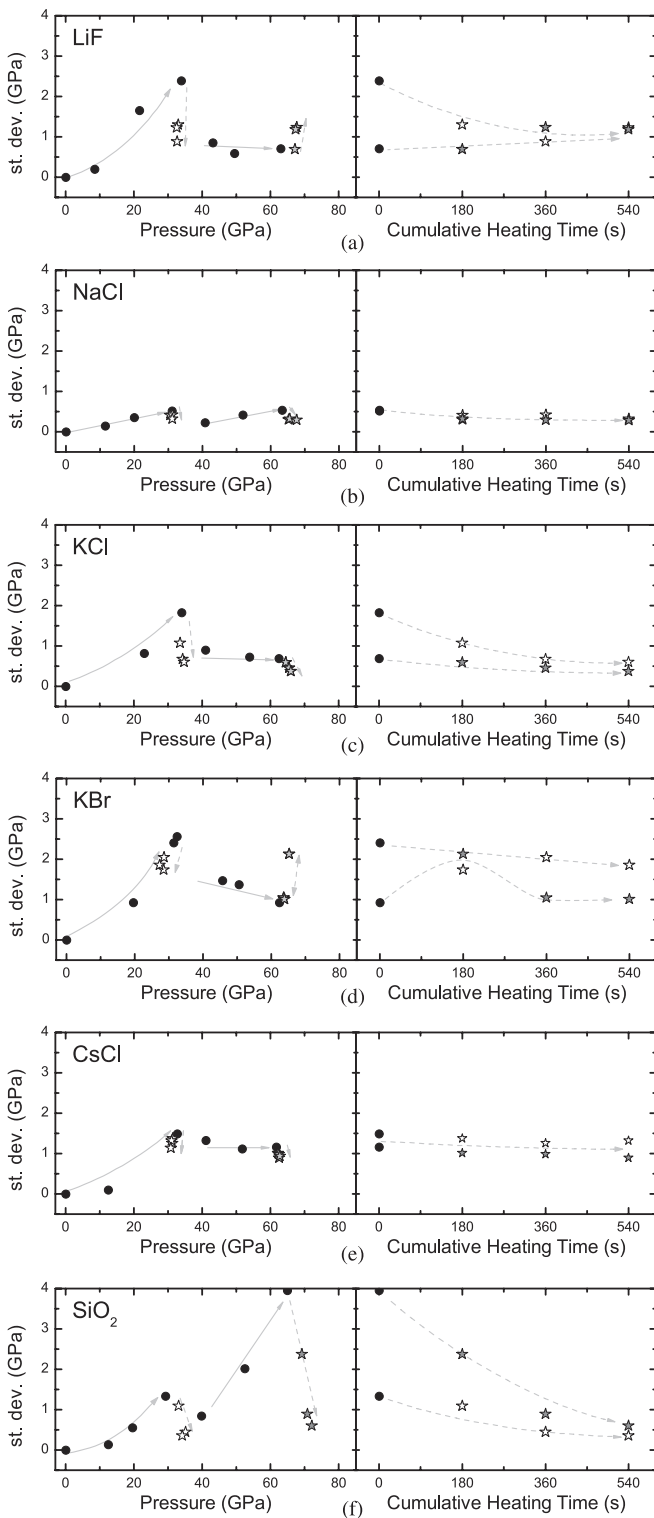


FIG. 2. Pressure gradients and annealing for pressure media: (a) LiF, (b) NaCl, (c) KCl, (d) KBr, (e) CsCl, and (f) α -SiO₂. (Left) Standard deviation of pressure versus average sample pressure without annealing (black circles) and following laser annealing (stars). (Right) Standard deviation versus heating duration at \sim 30 GPa (white stars) and at \sim 60 GPa (gray stars). Lines are guides for the eye.

Additionally, upon opening the DAC, we also observed a crack on the diamond culet surface that most likely emerged during one of the final annealings where we see a slight increase in the pressure standard deviation despite annealing.

B. NaCl

Much like the LiF sample, cold compression of the NaCl sample was accompanied by an increase in the standard deviation, albeit smaller. The standard deviation appears to increase linearly both before and after annealing on compression, with similar slopes (Fig. 2(b)). Annealing at \sim 30 GPa and \sim 60 GPa reduces the standard deviation within the sample; standard deviation appears to have decreased and stabilized with additional heating. Neither damage to the diamond anvils nor any gasket changes are observed during the compression and annealing of this sample.

C. KCl

We measure an increase in the standard deviation during the cold compression of the sample containing the KCl pressure medium foils. The first round of annealing at \sim 30 GPa significantly reduces the standard deviation within the sample (Fig. 2(c)). Post-heating compression appears to have slightly decreased the standard deviation within the sample by about half. Heating at \sim 60 GPa results in a decrease of the standard deviation as well. As with the NaCl sample, additional 3-min heating intervals appear to decrease the standard deviation and level off within the sample. Neither damage to the diamond anvils nor any gasket alterations are observed during the compression and annealing of this sample.

D. KBr

Standard deviation of the sample with KBr foils increases during cold compression. The pressure, in addition to the standard deviation, decreases during annealing of the sample (Fig. 2(d)). Post-heating compression appears to result in the decrease of the standard deviation, while annealing at \sim 60 GPa appears to first significantly increase the standard deviation within the sample, but to then return it to a value similar to the standard deviation of the sample at \sim 60 GPa prior to annealing. As with the LiF sample, an increase in the gasket hole diameter was observed during the second round of laser annealing and a fracture was found in one of the diamonds after the unloading of the sample.

E. CsCl

Cold compression of the CsCl pressure medium sample causes an increase in the standard deviation of the sample (with the greatest increase in standard deviation occurring during the 10–30 GPa increase in pressure) (Fig. 2(e)). Annealing slightly decreases the standard deviation at both \sim 30 GPa and \sim 60 GPa; however, the standard deviation does not appear to have significantly changed with heating duration. As the sample is compressed between \sim 30 GPa and \sim 60 GPa, standard deviation changes minimally. Neither defects of the diamond anvil culets nor any gasket alterations are observed during the compression and annealing of this sample.

F. α -SiO₂

Cold compression of amorphous SiO₂ pressure media foils is accompanied with an increase in the standard deviation of the sample. Annealing at ~ 30 GPa significantly reduced the standard deviation within the sample. Post-heating compression significantly increases the standard deviation in the sample to ~ 4 GPa, which is $\sim 33\%$ higher than the next highest standard deviation observed in DACs with any other pressure media that we have tested and may be due to the crystallization of the initially amorphous silica to its high-pressure stishovite form.¹² Annealing at ~ 60 GPa restores the standard deviation to similar values to those seen after annealing at ~ 30 GPa. Additional heating time, both at ~ 30 GPa and ~ 60 GPa, results in a decrease and eventual leveling off of the standard deviation within the sample, as is evident in Fig. 2(f).

G. Identification of diamond damage

In a few of our experiments, we damaged the anvils while laser heating at pressure. Diamond damage is common in high-pressure experiments and can occur as complete anvil failure, surface culet scratches, or internal fractures. As the Raman excitation laser travels through the anvil, it is possible to detect internal fractures (while still holding pressure, albeit at a usually reduced value) within an anvil as the diamond's stress state is compromised. Provided the fracture has not propagated in to the culet, the anvil can still withstand high pressures, although precariously. Comparing a clean, unfractured anvil at high pressures (Fig. 3) to a fractured anvil also at high pressures (Figs. 4 and 5), we find distinct topographical features in the Raman spectra. We find that for all of our anvils under high pressures ($> \sim 10$ GPa), the first-order Raman signal of the culet begins at ~ 1334 cm⁻¹, the same value of the anvil that is not under any confining pressure, regardless of pressure. The Raman spectra broadens with increased pressures, such that the edge of the spectrum gives the pressure of the sample attained.¹⁰ Other features include high Raman intensity at the location of internal fractures and could be used in the preliminary identification of fractures in diamond anvils or in cases when simultaneous optical identification is not possible.

The Raman signal of the diamond culet can be used to track expansion and propagation of internal diamond fractures at high pressures. Our study suggests that the first-order Raman signal of the diamond culet, when subjected to high pressures, can be used to extract a wealth of information. For example, we find the stress-strain distribution across the diamond culet, making it possible to measure the magnitude of the stress gradient between the culet edge and sample chamber (Figs. 4 and 5).

IV. DISCUSSION

We find that in absence of any anomalous behavior induced by laser heating (gasket hole expansion, shift, evolution of diamond cracks) all samples tested experience an increase in their standard deviation of pressure during cold

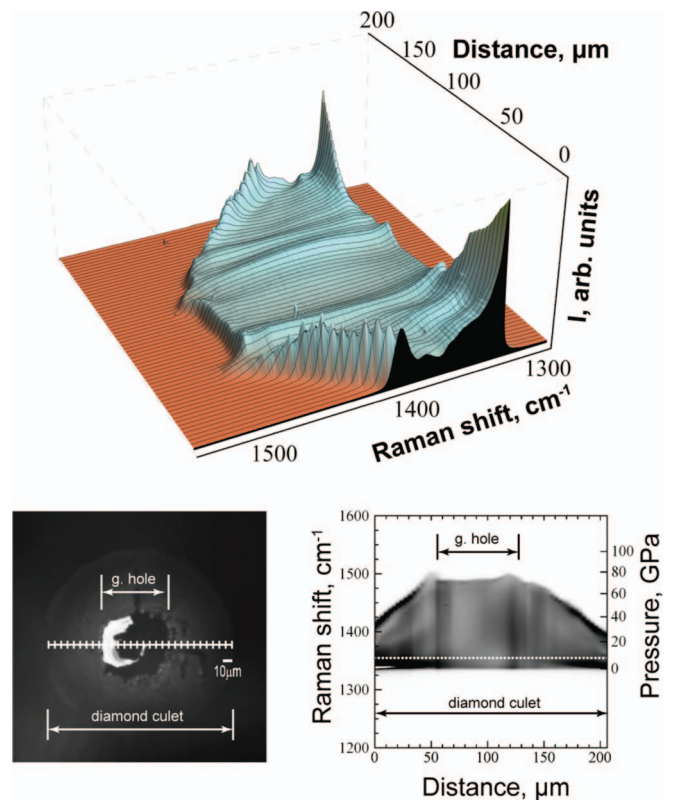


FIG. 3. Pressure variations across the culet at ~ 70 GPa, after laser annealing, for a pristine anvil. (Top) The diamond anvil first-order Raman spectra, and their relative intensities, across the diamond culet. Note that the full 3D figure is represented by a combination of the individual Raman spectra (same collection time) collected at evenly-spaced points across the culet. We show the Raman spectrum at the edge of diamond culet and emphasize it by black fill color. (Bottom, left) Photomicrograph of the diamond culet and sample as seen through the top diamond. (Bottom, right) 2D intensity map obtained by projecting Raman signal intensity to a Raman shift–distance plane and corresponding pressures. Pressure scale was determined relative to the ambient conditions Raman signal collected from the corresponding diamond anvil. Darker regions denote areas of higher intensity. The gasket hole (sample chamber) and diamond culet are labeled. Note the similarity of the Raman spectra at the middle of the diamond culet, corresponding to the gasket hole, hence the similarity of the corresponding pressures across the interior of the gasket hole.

compression and a reduction in their standard deviation of pressure during initial annealing at ~ 30 GPa. Standard deviation of pressure distribution in the sample is reduced with laser heating and becomes stable with additional heating time at ~ 30 GPa. Homogenization of pressure inside the sample chamber almost certainly takes place by diffusion-related processes. Although we cannot directly determine deviatoric stresses by our method, we are confident that these same processes also reduce both macro and micro deviatoric stresses within the sample. For the majority of pressure media (LiF, NaCl, KCl, CsCl, and α -SiO₂), the standard deviation either increases or remains the same with increasing pressure at room temperature after annealing at ~ 30 GPa. On the other hand, KBr behaves differently. We attribute the decrease in standard deviation within the KBr sample to fractures that likely formed during compression and are observed upon quenching. However, this behavior can also be explained in terms of material strength and annealing, which removes

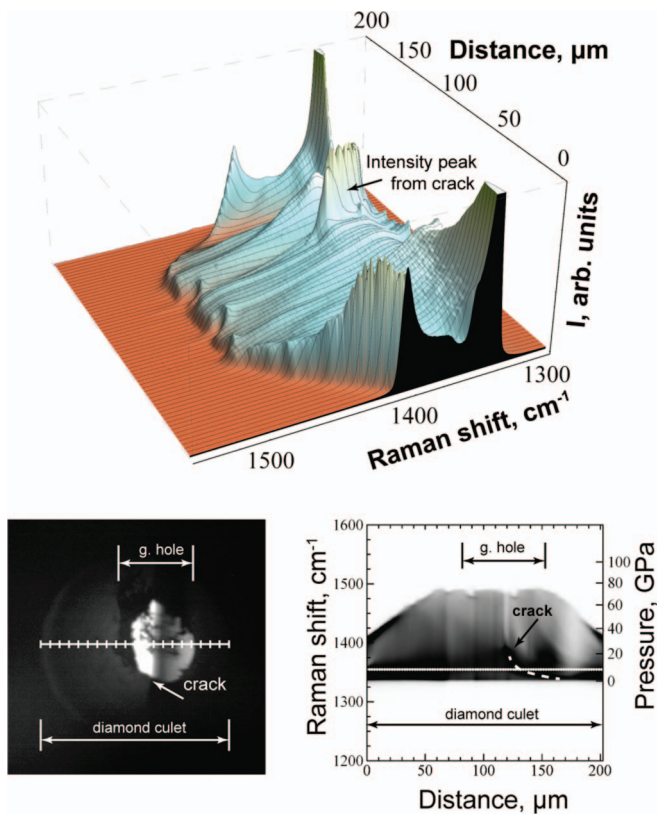


FIG. 4. Pressure variations across the culet at ~ 70 GPa, after laser annealing, of an internally fractured anvil. (Top) The diamond anvil first-order Raman spectra, and their relative intensities, across the diamond culet. Note that the full 3D figure is represented by a combination of the individual Raman spectra (same collection time) collected at evenly-spaced points across the culet. We show the Raman spectrum at the edge of diamond culet and emphasize it by black fill color. (Bottom, left) Photomicrograph of the diamond culet and sample as seen through the top diamond. (Bottom, right) 2D intensity map obtained by projecting Raman signal intensity to a Raman shift–distance plane and corresponding pressures. Pressure scale was determined relative to ambient conditions Raman signal collected from the corresponding diamond anvil. Darker regions denote areas of higher intensity. Note the high intensity of the Raman signal in the region of the internal crack, which was incurred during heating. The gasket hole (sample chamber) and diamond culet are labeled. Note the similarity of the Raman spectra at the middle of the diamond culet, hence the similarity of the corresponding pressure, across the interior of the gasket hole.

dislocations as agents of pressure gradients. Indeed, on the micro-scale, dislocations resist material flow and thus prevent homogeneous pressure distribution in the sample chamber. Finally, we find a reduction in the standard deviation of many samples (NaCl, KCl, CsCl, and α -SiO₂) following annealing at ~ 60 GPa. As at 30 GPa, KBr did not experience a reduction in its standard deviation again likely due to fractures of the diamond anvils and/or gasket expansion observed upon heating at ~ 60 GPa. The LiF sample also showed gasket hole expansion and a fracture of the diamond anvils annealed at ~ 60 GPa.

Following these results, we rank the solid pressure media that perform the best in terms of minimal pressure gradients without any laser annealing are: NaCl, CsCl, α -SiO₂, KCl, LiF, and KBr. Note that the last 2 in this ranking exhibited cracks upon quench; however, we do not expect any cracks to have formed on the anvils prior to heating at such low

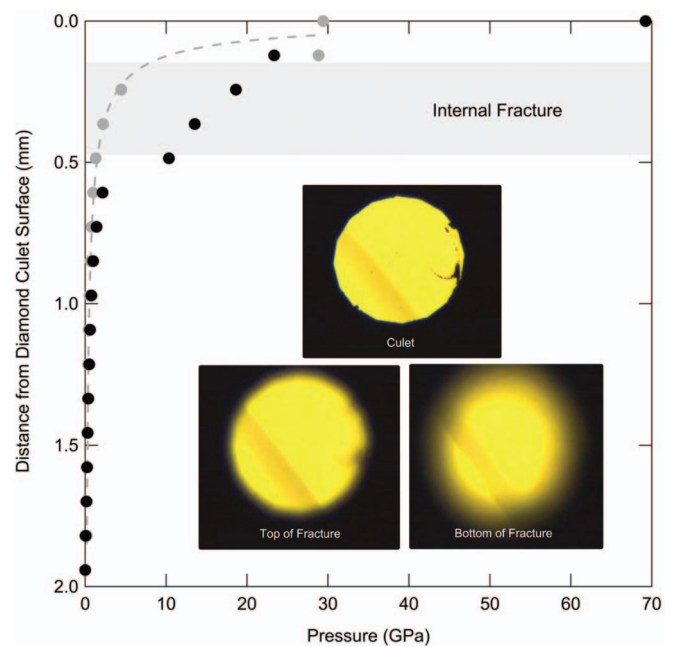


FIG. 5. A pressure versus depth profile of a pristine diamond anvil at ~ 30 GPa (gray circles) and an internally fractured anvil at ~ 70 GPa (black circles). The size of the internal fracture found (as denoted by a depth of ~ 300 μm) within the internally fractured anvil corresponds to the pressure discontinuity observed. Additionally, we show photomicrographs of the internally fractured anvil made at ambient conditions, namely, the culet surface, top of the fracture, and bottom of the fracture.

pressures (up to ~ 30 GPa). It is difficult to pinpoint when the fractures first manifested, but this may be one of the causes of pressure gradients as determined by diamond Raman. Additionally, sample geometry changes may also influence pressure gradients. In order to generalize our results, we mention that values shown in Fig. 2 can be normalized to ~ 50 μm , the furthest distance between measured points (see Fig. 1(b)).

We note that for each of the pressure media investigated, all show a significant drop in pressure gradients with just one heating: up to 50% drop in standard deviation for LiF, NaCl, KCl, and α -SiO₂. A smaller drop is measured for KBr and CsCl, although the drop in standard deviation is maintained under further cold compression.

In Table I, we list the corresponding room-pressure values for the melting temperature, bulk modulus K , and shear modulus G for the pressure media studied. We find no systematic trends based on these values, except that the large increase in standard deviation in SiO₂ after heating is suggestive of stishovite formation and as stishovite is rather hard (i.e., large K and G) in comparison to the alkali halides, a high standard deviation is expected. Like the rest of the materials studied however, upon laser annealing, this standard deviation is decreased.

If we compare our best solid cold-compressed pressure medium NaCl with other common pressure media such as cold-compressed inert gases, we find, that at 30 GPa, the standard deviations measured in NaCl are comparable to those found in Ar and N₂, but $5\times$ greater than that found in unannealed samples containing Ne and approximately an order of

magnitude greater than those measured in unannealed samples containing He.⁴

Our work on solid pressure media was conducted at 2000–3000 K; however, as we show in Fig. 2, time is nearly as important as temperature, especially for experiments anticipating high pressure–high temperature transitions and for experiments employing lower temperatures. Indeed, the Clapeyron slopes for such transitions can be both positive and negative, and pinpointing them requires precision in terms of pressure, temperature, and annealing duration, until the studied system achieves equilibrium. Additionally, it is important to realize that in a laser heating experiment pressure gradients are only reduced if there is good coupling of the laser with the absorber resulting in high temperatures and good heating of the sample and pressure media. In our experience, pressure media outermost to an absorber were not fully annealed.

Although hydrostaticity is critical in high-pressure experiments, there are other factors that are important to pressure medium choice and include interference of pressure medium signal with that of sample. For example, peak overlap in x-ray diffraction (XRD), Raman or FTIR measurements are undesirable. Likewise, as high-Z (i.e., more electrons) materials diffract better than comparably structured low-Z materials, the pressure medium is chosen to complement the sample such that the pressure medium does not overwhelm the signal of the sample. Phase transitions within a pressure medium are also an important factor in choosing pressure media. For example, the B1 → B2 phase transition in NaCl occurs at ~29 (±3) GPa (e.g., Refs. 13 and 14), whereas the same transition occurs at ~2 GPa for KCl and KBr.¹⁵ Sample reactivity with the pressure medium is also of crucial concern, especially at elevated temperatures where barriers to chemical reactions can be overcome. Additionally, materials with high melting temperatures help to prevent sample movement during experiments, thus minimizing geometrical changes in the gasket hole. Thus, with steadily expanding temperatures and pressures achievable by the diamond-anvil cell technique, it is crucial to have pressure media offering acceptable hydrostatic conditions based on these considerations.

V. CONCLUSIONS

As expected, our study shows that undesirable stresses around the sample are, in general, significantly reduced after laser annealing the sample. One may not assume, however, that heating always reduces these gradients because diamond-anvil fractures and changes in the size of the gasket hole can significantly increase these gradients. In the absence of these

two sources of error, we also find that heating the sample multiple times further minimizes the pressure gradients as we show for common solid pressure media, namely LiF, NaCl, KCl, CsCl, KBr, as well as amorphous SiO₂. Finally we emphasize the importance of time and annealing temperatures for minimization of pressure gradients inside the diamond anvil cell sample chamber.

ACKNOWLEDGMENTS

Portions of this work were funded by the Carnegie/DOE Alliance Center and the National Science Foundation (Grant No. EAR-0955824). We thank two anonymous reviewers for valuable feedback.

- ¹D. L. Decker, W. A. Bassett, L. Merrill, H. T. Hall, and J. D. Barnett, *J. Phys. Chem. Ref. Data* **1**, 773 (1972).
- ²A. Jayaraman, *Rev. Mod. Phys.* **55**, 65 (1983).
- ³T. Kenichi, P. C. Sahu, K. Yoshiyasu, and T. Yasuo, *Rev. Sci. Instrum.* **72**, 3873 (2001).
- ⁴S. Klotz, J. C. Chervin, P. Munsch, and G. Le Marchand, *J. Phys. D* **42**, 075413 (2009).
- ⁵S. Klotz, L. Paumier, G. Le Marchand, and P. Munsch, *High Press. Res.* **29**, 649 (2009).
- ⁶K. Takemura, *J. Appl. Phys.* **89**, 662 (2001).
- ⁷D. Andrault and G. Fiquet, *Rev. Sci. Instrum.* **72**, 1283 (2001).
- ⁸R. C. Liebermann, *High Press. Res.* **31**, 493 (2011).
- ⁹H. K. Mao, P. M. Bell, J. W. Shaner, and D. J. Steinberg, *J. Appl. Phys.* **49**, 3276 (1978).
- ¹⁰Y. Akahama and H. Kawamura, *J. Appl. Phys.* **100**, 043516 (2006).
- ¹¹Z. Du, G. Amulele, L. R. Benedetti, and K. K. M. Lee, *Rev. Sci. Instrum.* **84**, 075111 (2013).
- ¹²S. M. Stishov and N. V. Belov, *Dokl. Akad. Nauk SSSR* **143**, 951 (1962).
- ¹³Y. Sato-Sorensen, *J. Geophys. Res.* **88**, 3543, doi:10.1029/JB088iB04p03543 (1983).
- ¹⁴D. L. Heinz and R. Jeanloz, *Phys. Rev. B* **30**, 6045 (1984).
- ¹⁵A. Dewaele, A. B. Belonoshko, G. Garbarino, F. Occelli, P. Bouvier, M. Hanfland, and M. Mezouar, *Phys. Rev. B* **85**, 214105 (2012).
- ¹⁶*CRC Handbook of Chemistry and Physics*, edited by D. R. Lide (CRC Press, Boca Raton, FL, 1990), Vol. 71.
- ¹⁷R. Boehler, M. Ross, and D. B. Boercker, *Phys. Rev. Lett.* **78**, 4589 (1997).
- ¹⁸D. L. Anderson, *New Theory of the Earth* (Cambridge University Press, Cambridge, 2007).
- ¹⁹A. J. Campbell and D. L. Heinz, *J. Phys. Chem. Solids* **52**, 495 (1991).
- ²⁰L. S. Combes, S. S. Ballard, and K. A. McCarthy, *J. Opt. Soc. Am.* **41**, 215 (1951).
- ²¹A. Polian, D. Vo-Thanh, and P. Richet, *Europhys. Lett.* **57**, 375 (2002).
- ²²D. J. Weidner, J. D. Bass, A. E. Ringwood, and W. Sinclair, *J. Geophys. Res.* **87**, 4740, doi:10.1029/JB087iB06p04740 (1982).
- ²³G. A. Lyzenga, T. J. Ahrens, and A. C. Mitchell, *J. Geophys. Res.* **88**, 2431, doi:10.1029/JB088iB03p02431 (1983).
- ²⁴F. Birch, *J. Geophys. Res.* **57**, 227, doi:10.1029/JZ057i002p00227 (1952).
- ²⁵P. Vinet, J. Ferrante, J. H. Rose, and J. R. Smith, *J. Geophys. Res.* **92**, 9319, doi:10.1029/JB092iB09p09319 (1987).
- ²⁶P. Richet, Y. Bottinga, J. P. Petitet, and C. Tequi, *Geochim. Cosmochim. Acta* **46**, 2639 (1982).